Int. J. Electrochem. Sci., 15 **(2020)** 3274 – 3282, doi: 10.20964/2020.04.01

International Journal of
ELECTROCHEMICAL
SCIENCE
www.electrochemsci.org

Short Communication

Ni-Au Anodic Nano-Electrocatalyst for Direct Glucose Fuel Cells

Aya S. Abdulhalim[1], *Yasser M. Asal*[1], *Ahmad M. Mohammad*[2*], *Islam M. Al-Akraa*[1,*]

[1] Department of Chemical Engineering, Faculty of Engineering, The British University in Egypt, Cairo 11837, Egypt
[2] Chemistry Department, Faculty of Science, Cairo University, Cairo 12613, Egypt
[*]E-mails: islam.ahmed@bue.edu.eg (Islam M. Al-Akraa); ammohammad@cu.edu.eg (Ahmad M. Mohammad)

Received: 21 October 2019 / *Accepted:* 28 December 2019 / *Published:* 10 March 2020

This study aims at the sequential assembling of a nickel oxide (NiOx: cauliflower-like nanostructure, 90 nm) and gold (Au; spherical, 95 nm in an average particle size) onto the GC surface nanocatalyst on a glassy carbon (GC) electrode (will be abbreviated as Ni-Au/GC) for the glucose electro–oxidation (GO); the principal anodic reaction in the direct glucose fuel cells (DGFCs). The charge of the Ni deposition on the GC surface (will be abbreviated as Ni/GC electrode) was initially optimized to obtain the highest catalytic activity toward GO which attained at (339.8 Ag^{-1}) by applying 15 mC in the Ni deposition. Yet, the NiOx/GC could not maintain an enduring stability toward GO, which suggested a further modification with Au. Interestingly, this modification obviously improved the stability toward GO; sustaining the rate of current decay at the Ni-Au/GC catalyst much lower than that at the Ni/GC catalyst. After 1 h of continuous electrolysis, the current was 1.15 mA at the Ni-Au/GC electrode compared to 0.6 mA at the Ni/GC electrode (~ twofold higher).

Keywords: Glucose electro-oxidation; Ni; Au; Catalytic activity; Stability.

1. INTRODUCTION

With the strict measures and critical actions toward climate change, it has not become wise to invest more money in fossil fuels-based industries, although relatively cheaper than renewable energy. For example, in Egypt, research proposals are calling to sustain the industry of electric vehicles rather to continue working with diesel-based cars. Also, the local government is encouraging the private sector to get involved in this technology, paving the road for them with surpassing facilities and flexible marketing promises [1]. In fact, continuing more with fossil fuels combustions, even if fossil fuels remained unexhausted, would emit extensively harmful carbon, sulfur and nitrogen-containing

emissions to the atmosphere; influencing more the global warming. The rapidly growing increase in the world population also calls to finding new alternative resources for power generation capable to fulfil the advanced luxurious needs of people and the industrial revolution in developing countries [2-4].

In this regard, fuel cells (FCs) with their greenness, enhanced efficiency, reliability, moving flexibility stands as a promising industry for a wide range of electrical portable and stationary applications [5-15]. The big names vehicles' companies of as Honda, Toyota and Nissan are now switching their production toward the fuel cell vehicles (FCVs) which exhibited much less emissions and higher efficiencies than diesel-based cars. The name "Mirai" that has been chosen by Toyota means “future” in the Japanese language where it reflects the potential of FCVs achieving sustainable mobility and energy diversification [16]. Mostly, the H_2/O_2 FCs are employed for this industry but the expensive cost of miniaturizing the H_2 containers and the safety concerns of working with H_2 has steered the effort to employ rather a liquid fuel.

Glucose as a natural sugar that can easily be extracted from green crops, such as leaves, grasses, legumes, stems of green plants and tree leaves [17] and as a non-toxic material represented an ideal choice as fuel in FCs. For long time, the glucose fuel cells (GFCs) depended on the glucose electro−oxidation (GO) with enzymes and microbes but both showed very poor performances with undesired durability [1, 18-23]. This was originated from the limited life-time of enzymes and the sluggish electron transfer from the microbe to the electrode [21, 23-25]. On the other hand, the direct GO on noble metals and metal oxides; particularly, on Au and Au composites, met a desirable satisfaction [24]. Chen *et al*. has recently reported an enhanced GO on A three-dimensional Au/Ni foam electrodes that resulted a glucose fuel cell with a power density of 26.6 mW cm^{-2} at 89 mA cm^{-2} (0.5 M glucose and 6 M KOH) at a temperature of 70 °C, which was favorable for large-scale production [18].

Herein, we report on the fabrication of a Ni-Au/GC modified catalyst that owned an attractive improved catalytic activity toward GO. The layer-by-layer electrodeposition as a cheap, controllable and facile strategy for assembling hybrid nanocatalysts was employed in the catalyst's preparation. With this catalyst, a catalytic efficiency for GO up to 339.8 Ag^{-1} was attained.

2. EXPERIMENTAL

A mechanically–polished glassy carbon (d = 5.0 mm), An Ag/AgCl/KCl(sat) and a spiral Pt wire were used as working, reference and counter electrodes, respectively.

The GC modification with NiOx was carried out in two consecutive steps. The first one is the deposition of metallic nickel from an aqueous solution of 0.1 M acetate buffer solution (ABS, pH = 4.0) containing 0.1 M $NiSO_4$ by a constant potential electrolysis at −1 V. Then, the metallic Ni was oxidized in 0.1 M phosphate buffer solution (PBS, pH = 7) by scanning the potential between − 0.5 and 1 V for 10 cycles at 100 mV s^{-1}. On the other side, the GC modification with Au was carried out in 0.1M H_2SO_4 solution containing 1.0 mM $NaAuCl_4$ at a constant potential of 0.1 V for 5 min.

The electrochemical measurements were carried out in a traditional three-electrode glass cell at room temperature (around 25 °C) using a BioLogic SAS potentiostat (model SP-150) operated with EC-lab® software. The catalytic performance of the modified electrodes towards GO was investigated in 0.5 M NaOH solution containing 50 mM glucose.

A scanning electron microscope (SEM, Joel GSM-6610LV, Japan) joined with an energy dispersive X-ray spectrometer (EDS, with accelerating voltage 30 K.V with original magnification ×500, ISIS Company, Oxford, England) was engaged to determine the electrode surface morphology and composition, respectively. The crystal structure of the modified Ni-Au/GC electrode is identified using XRD (PANalyticalX'Pert PRO instrument, Cu Kα radiation (λ = 1.5404 Å).

3. RESULTS AND DISCUSSION

3.1. Electrochemical characterization

Figure 1 shows CVs obtained at (a) bare GC, (b) Ni/GC and (c) Ni-Au/GC electrodes. The measurements are carried out in an alkaline medium to properly monitor the oxidation/reduction behavior of the electrodeposited Ni at the GC surface. At the bare GC electrode (Fig. 1a), no typical response was observed under the current experimental conditions. But for the Ni/GC (Fig. 2b) and Ni-Au/GC (Fig. 2c) electrodes, a redox couple attributed to the transformation between the $Ni(OH)_2$ and the NiOOH oxidation states of Ni [26] is monitored at 0.45 and 0.25 V. Another cathodic peak has been observed at ca. 0.15 V for the Ni-Au/GC electrode related to the Au oxide reduction [15]. This confirms the successful deposition of Ni and Au over the GC surface.

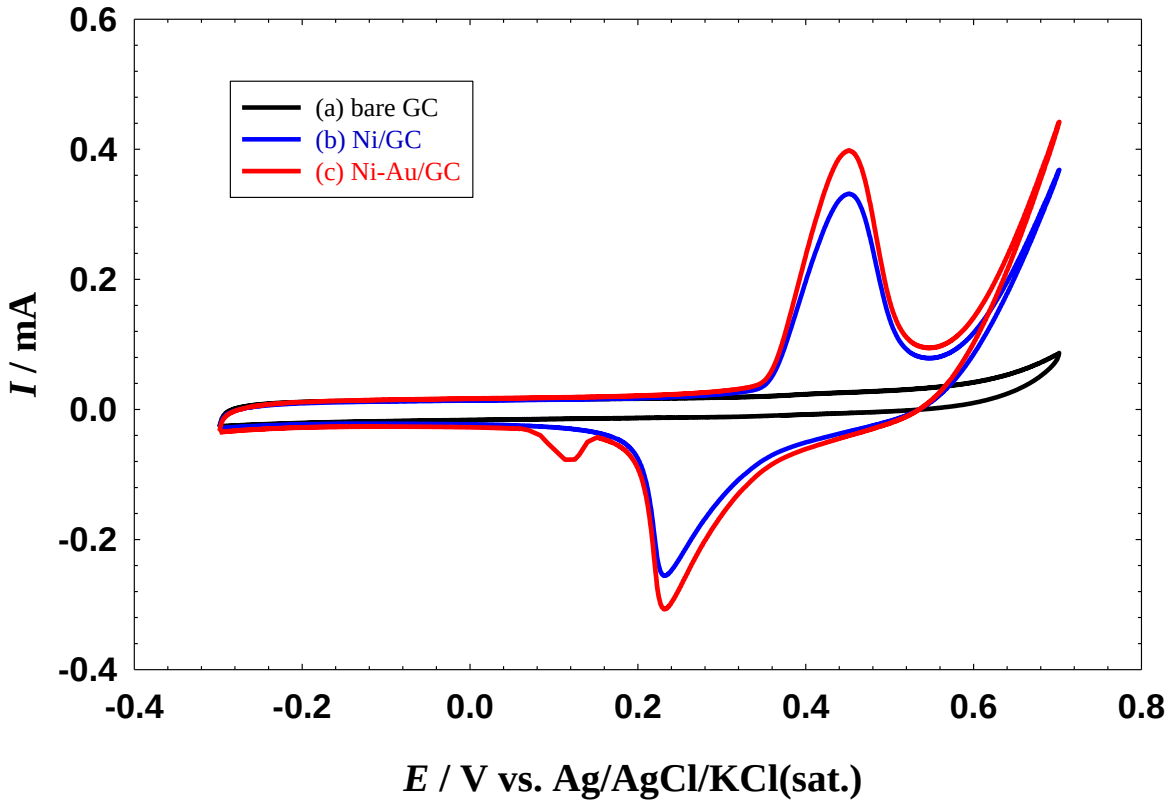

Figure 1. CVs measured in 0.5 M NaOH solution at a scan rate of 100 mVs^{-1} for (a) the bare GC electrode, (b) the Ni/GC and (c) the Ni-Au/GC electrodes at which a 15 mC of Ni has been applied during the electrodeposition

3.2. Material characterization

Morphologically, Fig. 2A and B shows FE-SEM images of the Ni/GC and Ni-Cu/GC electrodes at which a 15 mC of Ni has been applied during the electrodeposition, respectively. Both figures show a clear view about the deposition of the NiOx at the GC surface in a 90 nm cauliflower-like structure. On the other hand, Fig. 2B shows the deposition of spherical Au onto the GC surface with an average particle size of 95 nm.

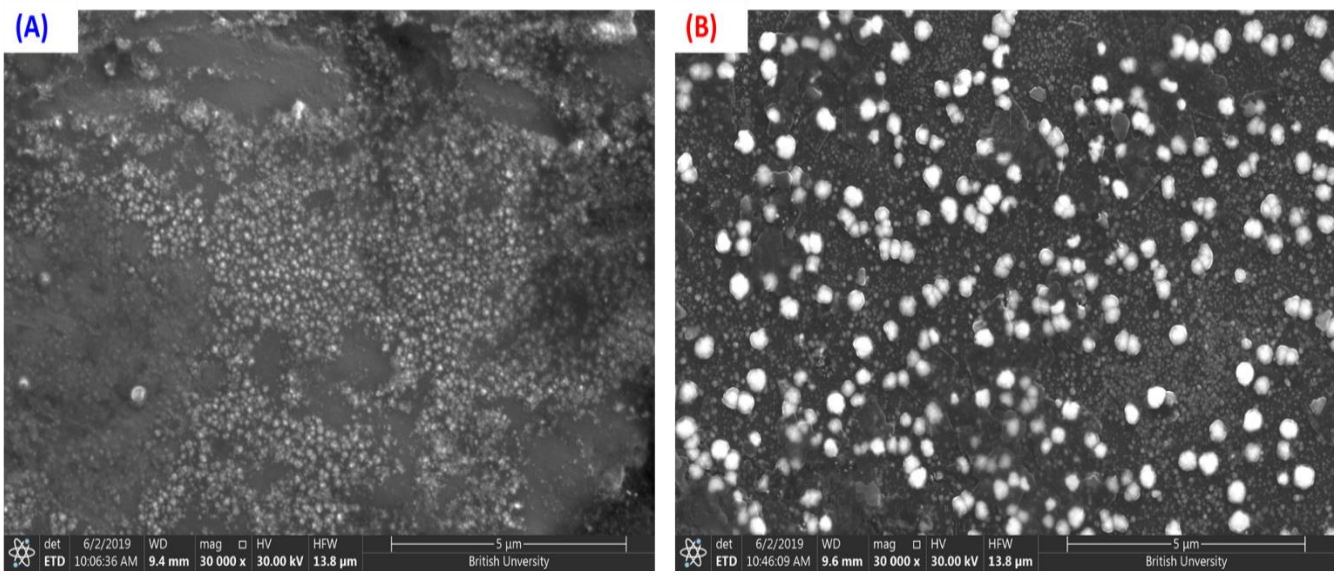

Figure 2. SEM images of the (A) Ni/GC and (B) Ni-Au/GC electrodes at which a 15 mC of Ni has been applied during the electrodeposition.

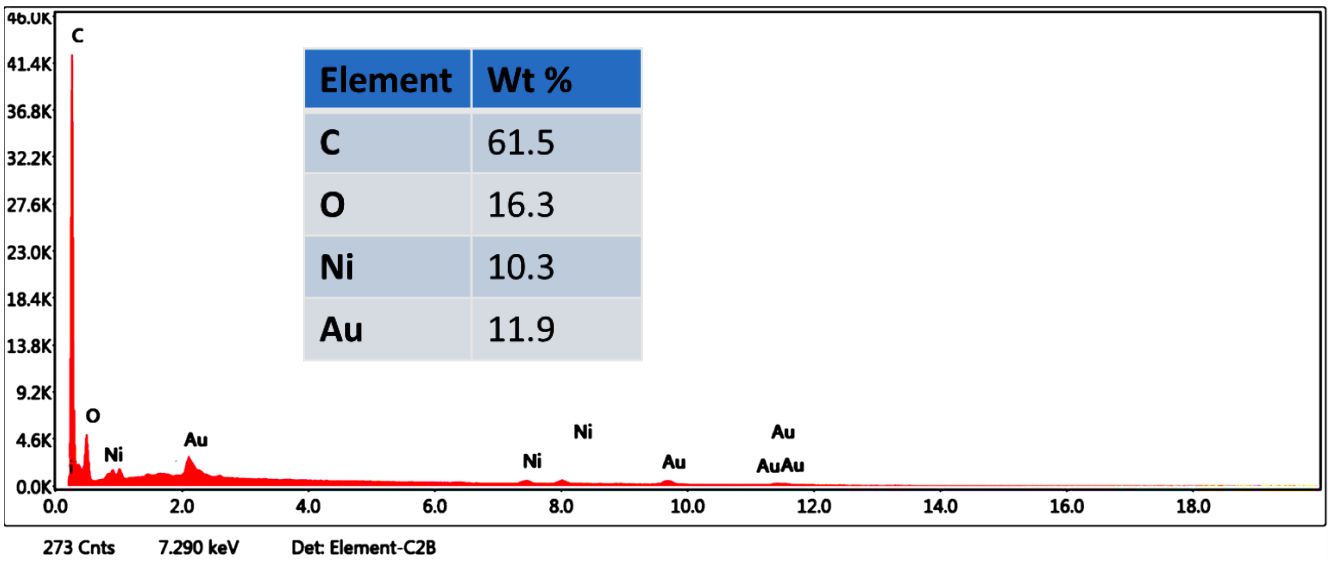

Element	Wt %
C	61.5
O	16.3
Ni	10.3
Au	11.9

Figure 3. EDS analysis of the Ni-Au/GC electrodes at which a 15 mC of Ni has been applied during the electrodeposition.

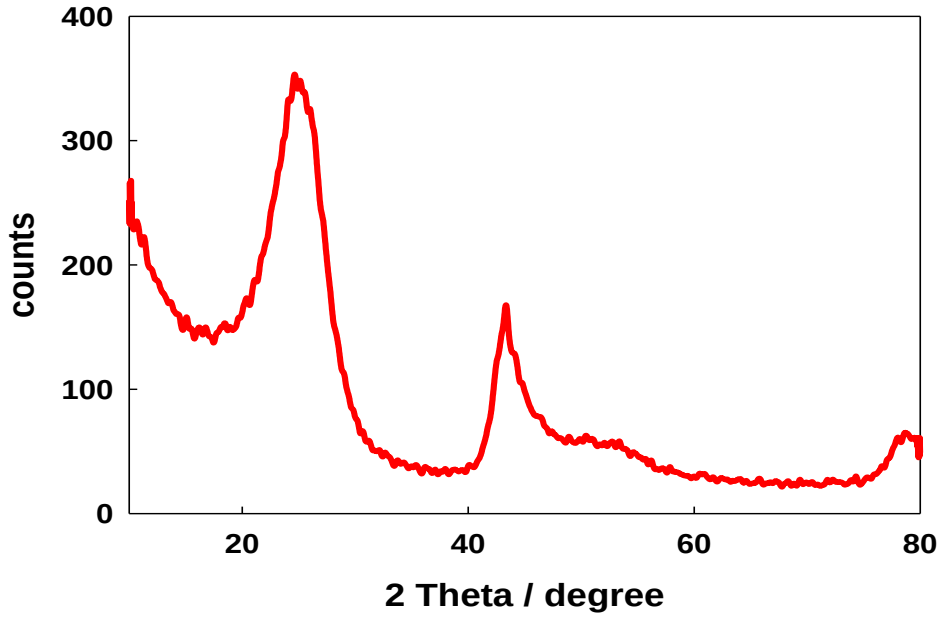

Figure 4. XRD analysis of the Ni-Au/GC electrodes at which a 15 mC of Ni has been applied during the electrodeposition.

The EDS analysis in Fig. 3 confirmed the successful deposition of the catalyst components and aided in calculation of their relative ratios. The peaks of C, O, Ni and Au appeared at their allocated positions and their relative ratios appears in the table inserted as inset of Fig. 3.

Moreover, the XRD analysis assisted in identifying the crystal structure of the Ni-Au/GC electrode as shown in Fig. 4. The broad peaks at ca. 2θ 25^{o} and 78 ^{o} are related to the glassy carbon support. The three sharp peaks appeared at ca. 43.3^{o}, 50.6^{o} and 74.2^{o} are related to Ni (111), (002) and (022) planes of Ni [21] and no peaks were observed for Au which might result from alloying Au in the Ni lattice [13].

3.2. Electrocatalysis of GO

Figure 5 shows CVs of GO in 0.5 M NaOH containing 50 mM glucose at the (a) bare GC electrode and (b-f) Ni/GC electrodes with different deposition charge (Q) of Ni. Herein, it is valuable to say that the unmodified GC electrode (Fig. 5a) did not show any electrocatalytic activity towards GO under the current experimental conditions which agrees with previous investigations [21]. At the Ni/GC modified electrodes (Fig. 5b-f), the following interesting points appear:

(i) Glucose is easily oxidized, reflected from the anodic peak, indicating that the NiOx is a suitable catalyst for GO. It is expected that glucose is initially adsorbed at the active sites of NiOx and further oxidized to gluconolactone at higher potential at the same time with the transformation of $Ni(OH)_2$ to NiOOH [21]. So, NiOx here is acting as a catalytic mediator facilitating the GO (Eqs. 1 and 2).

$$Ni^{2+} \longrightarrow Ni^{3+} + e^{-} \quad (1)$$

$$Ni^{3+} + \text{glucose} \longrightarrow \text{gluconolactone} + Ni^{2+} \quad (2)$$

(ii) As the Ni deposition charge increasing, the current of the GO anodic peak around 0.6-0.8 V also increasing (Figs. 5b-f). This is because of increasing the number of active sites available for glucose adsorption.

(iii) Normalizing the current to the deposited mass, calculated from Faraday's law of electrolysis, utilizing the deposition charge, results in obtaining the highest specific current (339.76 A g^{-1}) when a 15 mC of Ni has been applied during the electrodeposition at the GC electrode as appearing from the inset of Fig. 5. This surpasses the values obtained at other reported catalysts (PtPd/graphene aerogel/nickel foam composite, Pd/C and Fe-Ni-Co/C) in literature [27, 28].

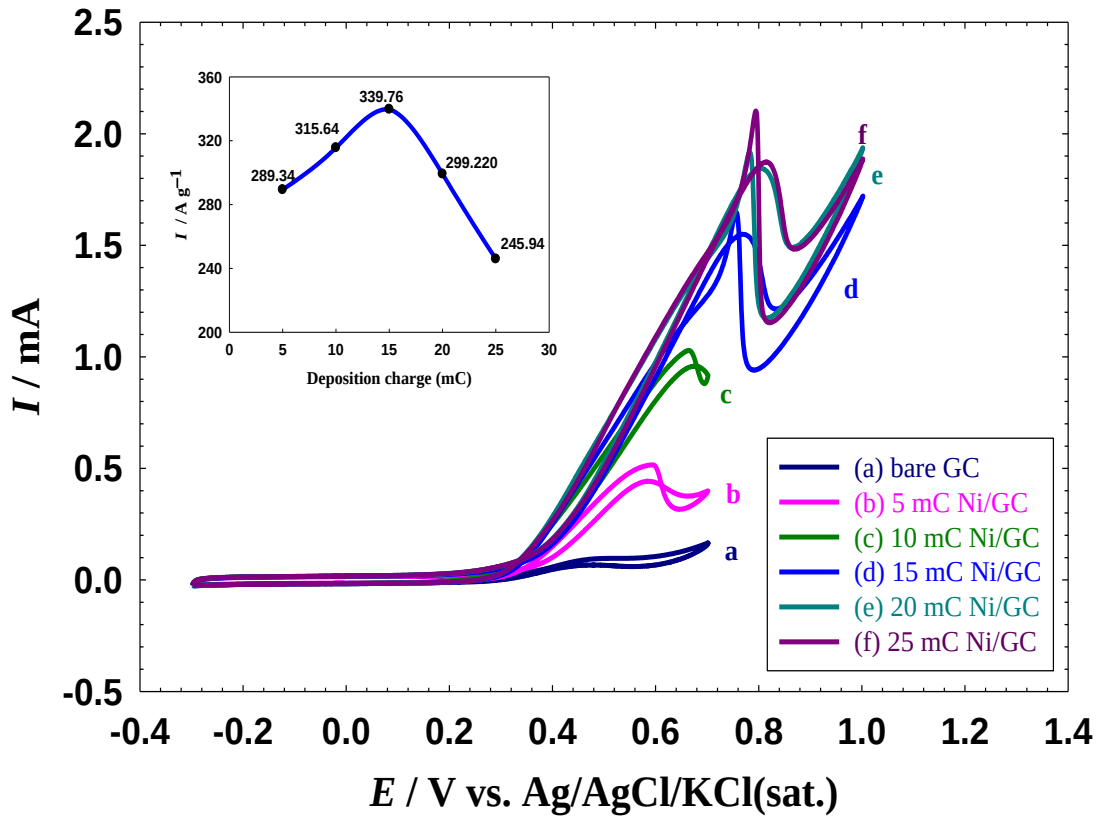

Figure 5. CVs measured in 0.5 M NaOH solution containing 50 mM glucose at a scan rate of 100 mVs^{-1} for (a) bare GC electrode and (b-f) Ni/GC electrodes with different deposition charge (Q) of Ni. The inset shows the specific current vs. the deposition charge of Ni.

Furthermore, aiming to improve the stability towards GO, the Ni/GC electrode has been modified with Au and the anodic current of GO has been recorded at a constant potential of 0.6 V for 1 h of

continuous electrolysis at the Ni/GC (Fig. 6a) and Ni-Au/GC (Fig. 6b) electrodes. Interestingly, the Ni-Au/GC electrode showed a better stability in terms of keeping a lower current decay during the continuous electrolysis. After 1 h of continuous electrolysis, the current maintained at 1.15 mA at the Ni-Au/GC electrode (Fig. 6b) compared with 0.6 mA at the Ni/GC electrode (Fig. 6a). This enhancement is supposed to arise from enhancing the mechanical properties of Ni and an improved the oxidation process of glucose with the deposition of Au because of its, specifically, and the nanostructures, generally, fascinating properties [29-37].

4. CONCLUSION

A novel binary catalyst composed of NiOx and Au has been assembled onto the GC electrode for the efficient GO. The deposition charge of Ni onto the GC electrode influenced, to a great extent, the catalytic efficiency. The highest catalytic activity was obtained at the Ni/GC electrode (at which a 15 mC of Ni has been applied during the electrodeposition). Moreover, a further modification of the Ni/GC electrode with Au increased the catalytic efficiency towards GO by ca. 2 folds. The enhancement in the electrocatalytic activity and stability is thought to arise from enhancing the mechanical properties of Ni and an improved the oxidation process of glucose with the deposition of Au.

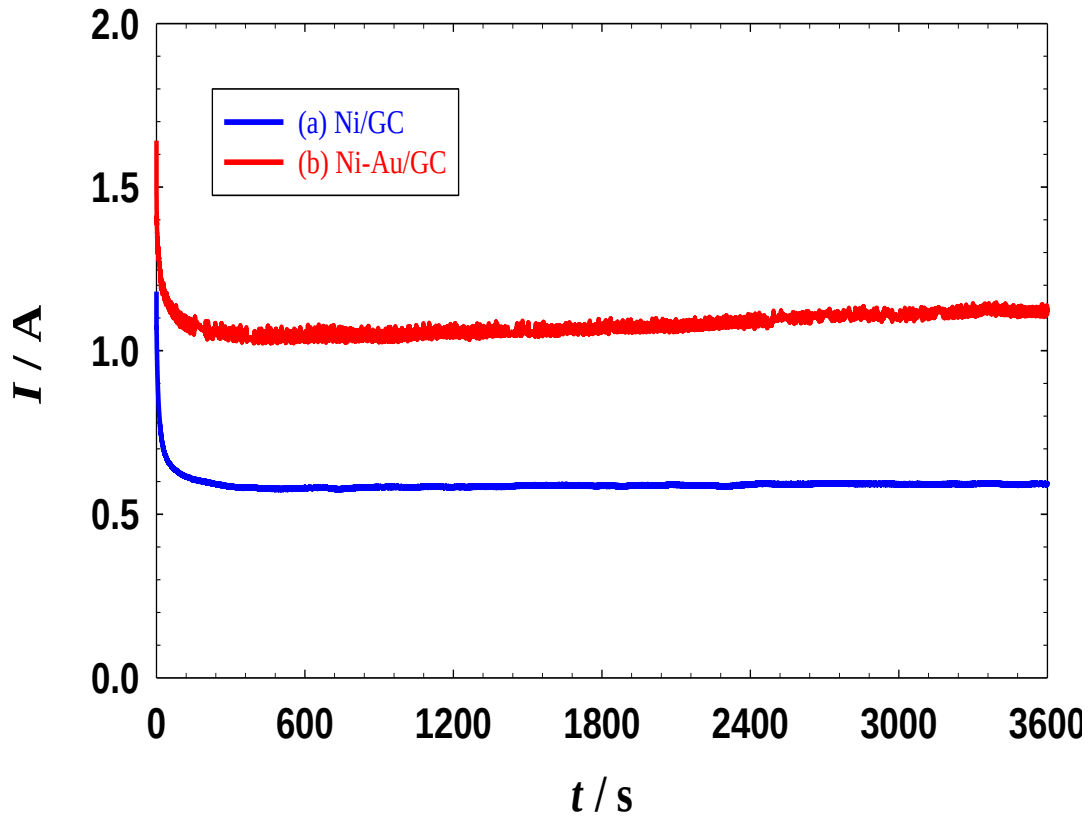

Figure 6. Current-time relation measured in 0.5 M NaOH solution containing 50 mM glucose at a constant potential of 0.6 V for (a) Ni/GC and (b) Ni-Au/GC electrodes at which a 15 mC of Ni has been applied during the electrodeposition.

References

1. D. Bissada. (Export.gov, 2019), https://www.export.gov/article?id=Egypt-Renewable-Energy .
2. I. M. Al-Akraa, A. M. Mohammad, M. S. El-Deab, B. E. El-Anadouli, *Int. J. Electrochem. Sci.*, 8 (2013) 458.
3. I. M. Al-Akraa, A. M. Mohammad, M. S. El-Deab, B. E. El-Anadouli, *Arab. J. Chem.*, 10 (2017) 877.
4. I. M. Al-Akraa, T. Ohsaka, A. M. Mohammad, *Arab. J. Chem.*, 12 (2019) 897.
5. I. M. Al-Akraa, *Int. J. Hydrogen Energy*, 42 (2017) 4660.
6. I. M. Al-Akraa, Y. M. Asal, A. M. Mohammad, *J. Nanomater.*, 2019 (2019)
7. I. M. Al-Akraa, A. M. Mohammad, M. S. El-Deab, B. E. El-Anadouli, *Int. J. Electrochem. Sci.*, 7 (2012) 3939.
8. I. M. Al-Akraa, A. M. Mohammad, M. S. El-Deab, B. E. El-Anadouli, *J. Electrochem. Soc.*, 162 (2015) F1114.
9. I. M. Al-Akraa, A. M. Mohammad, M. S. El-Deab, B. E. El-Anadouli, *Int. J. Hydrogen Energy*, 40 (2015) 1789.
10. I. M. Al-Akraa, A. M. Mohammad, M. S. El-Deab, B. E. El-Anadouli, in *Progress in Clean Energy, Volume 1: Analysis and Modeling*. (2015), pp. 551-558.
11. I. M. Al-Akraa, A. M. Mohammad, M. S. El-Deab, B. S. El-Anadouli, *Int. J. Electrochem. Sci.*, 10 (2015) 3282.
12. A. E. ALvarez, D. R. Salinas, *Electrochim. Acta*, 55 (2010) 3714.
13. Y. M. Asal, I. M. Al-Akraa, A. M. Mohammad, M. S. El-Deab, *Int. J. Hydrogen Energy*, 44 (2019) 3615.
14. Y. M. Asal, I. M. Al-Akraa, A. M. Mohammad, M. S. El-Deab, *J. Taiwan Inst. Chem. Eng.*, 96 (2019) 169.
15. A. M. Mohammad, I. M. Al-Akraa, M. S. El-Deab, *Int. J. Hydrogen Energy*, 43 (2018) 139.
16. H. Yumiya, *World Electric Vehicle Journal*, 7 (2015) WEVJ7.
17. M. H. Brown, in *https://patents.google.com/patent/US4359532A/en*. (USA, 1980), vol. US4359532A.
18. J. Chen, H. Zheng, J. Kang, F. Yang, Y. Cao, M. Xiang, *RSC Advances*, 7 (2017) 3035.
19. R. A. Bullen, T. C. Arnot, J. B. Lakeman, F. C. Walsh, *Biosens. Bioelectron.*, 21 (2006) 2015.
20. M. Ghasemi, M. Ismail, S. K. Kamarudin, K. Saeedfar, W. R. W. Daud, S. H. A. Hassan, L. Y. Heng, J. Alam, S. E. Oh, *Appl. Energy*, 102 (2013) 105.
21. A. M. Ahmed, S. Y. Sayed, G. A. El-Nagar, W. M. Morsi, M. S. El-Deab, B. E. El-Anadouli, *J. Electroanal. Chem.*, 835 (2019) 313.
22. P. Pandey, V. N. Shinde, R. L. Deopurkar, S. P. Kale, S. A. Patil, D. Pant, *Appl. Energy*, 168 (2016) 706.
23. S. Shleev, J. Tkac, A. Christenson, T. Ruzgas, A. I. Yaropolov, J. W. Whittaker, L. Gorton, *Biosens. Bioelectron.*, 20 (2005) 2517.
24. J. Chen, H. Zheng, J. Kang, F. Yang, Y. Cao, M. Xiang, *RSC Adv.*, 7 (2017) 3035.
25. K. Rabaey, N. Boon, S. D. Siciliano, M. Verhaege, W. Verstraete, *Appl. Environ. Microbiol.*, 70 (2004) 5373.
26. I. M. Al-Akraa, Y. M. Asal, S. D. Khamis, *Int. J. Electrochem. Sci.*, 13 (2018) 9712.
27. C.-H. A. Tsang, K. N. Hui, K. S. Hui, Electrochim. Acta, 258 (2017) 371.
28. M. Zhiani, A. Abedini, S. Majidi, Electrocatalysis, 9 (2018) 735.
29. B. A. Al-Qodami, H. H. Farrag, S. Y. Sayed, N. K. Allam, B. E. El-Anadouli, A. M. Mohammad, *J. Nanotechnol.*, 2018 (2018).
30. M. S. El-Deab, G. A. El-Nagar, A. M. Mohammad, B. E. El-Anadouli, *J. Power Sources*, 286 (2015) 504.

31. G. A. El-Nagar, M. S. El-Deab, A. M. Mohammad, B. E. El-Anadouli, *Electrochim. Acta*, 180 (2015) 268.
32. A. M. Mohammad, A. I. Abdelrahman, M. S. El-Deab, T. Okajima, T. Ohsaka, *Colloids Surf. A Physicochem. Eng. Asp.*, 318 (2008) 78.
33. A. M. Mohammad, S. Dey, K. K. Lew, J. M. Redwing, S. E. Mohney, *J. Electrochem. Soc.*, 150 (2003) G577.
34. A. M. Mohammad, T. A. Salah Eldin, M. A. Hassan, B. E. El-Anadouli, *Arab. J. Chem.*, 10 (2017) 683.
35. I. M. Sadiek, A. M. Mohammad, M. E. El-Shakre, M. S. El-Deab, B. E. El-Anadouli, J. *Solid State Electrochem.*, 17 (2013) 871.
36. I. M. Al-Akraa, A. M. Mohammad, *Arab. J. Chem.*, in press (2019) https://doi.org/10.1016/j.arabjc.2019.10.013.
37. I. M. Al-Akraa, A. M. Mohammad, M. S. El-Deab, B. E. El-Anadouli, *J. Nanotechnol.*, 2018 (2018).